

Supporting Information for:

On the Nature of Inter-Anion Coinage Bonds

Jiayao Li^[a], Qiuyan Feng^[a], Changwei Wang^{[a]} and Yirong Mo^{*[b]}*

^[a] Key Laboratory for Macromolecular Science of Shaanxi Province, School of Chemistry & Chemical Engineering, Shaanxi Normal University, Xi'an 710119, China.

^[b] Department of Nanoscience, Joint School of Nanoscience and Nanoengineering, University of North Carolina at Greensboro, Greensboro, NC 27401, USA.

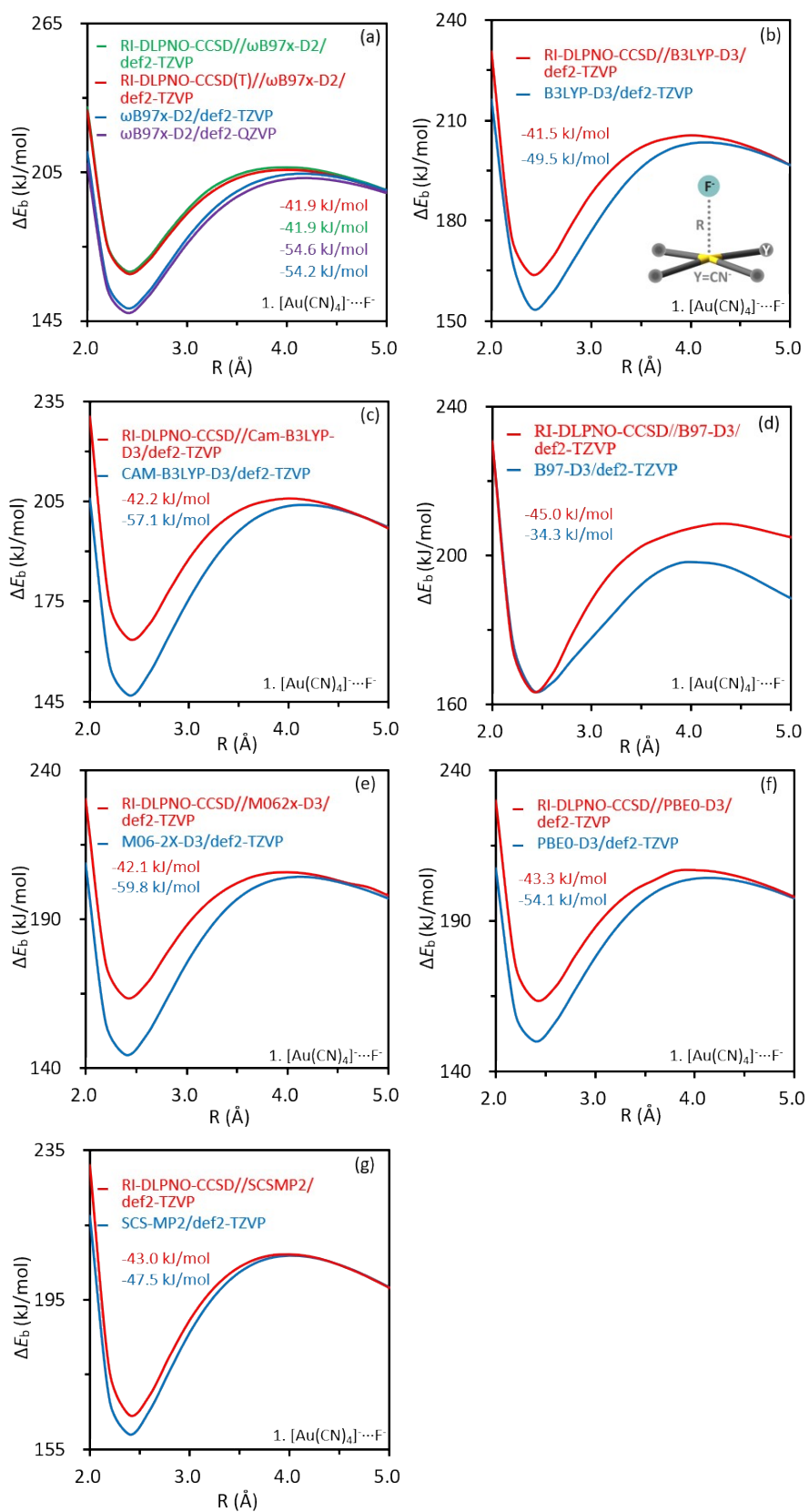
AUTHOR INFORMATION

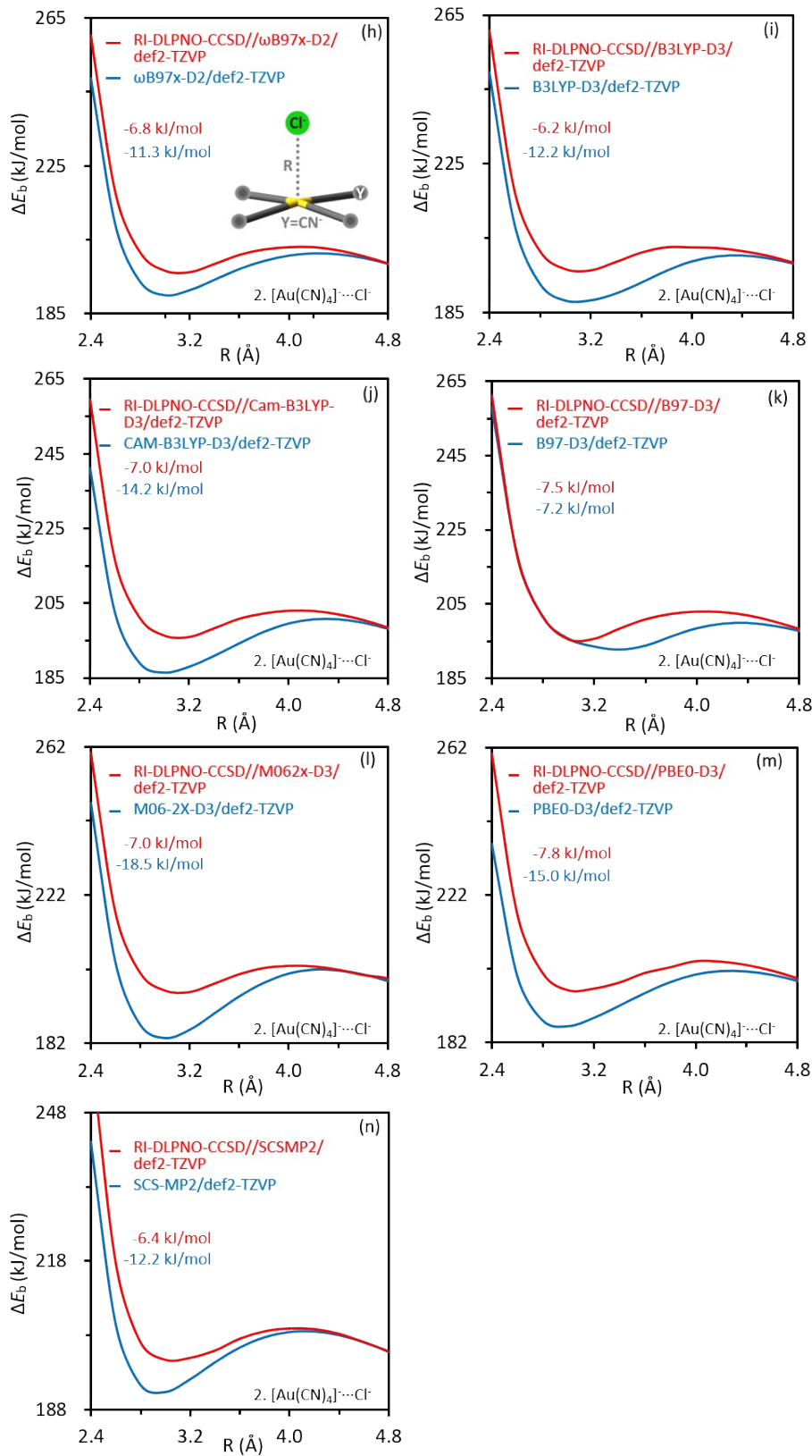
Corresponding Author

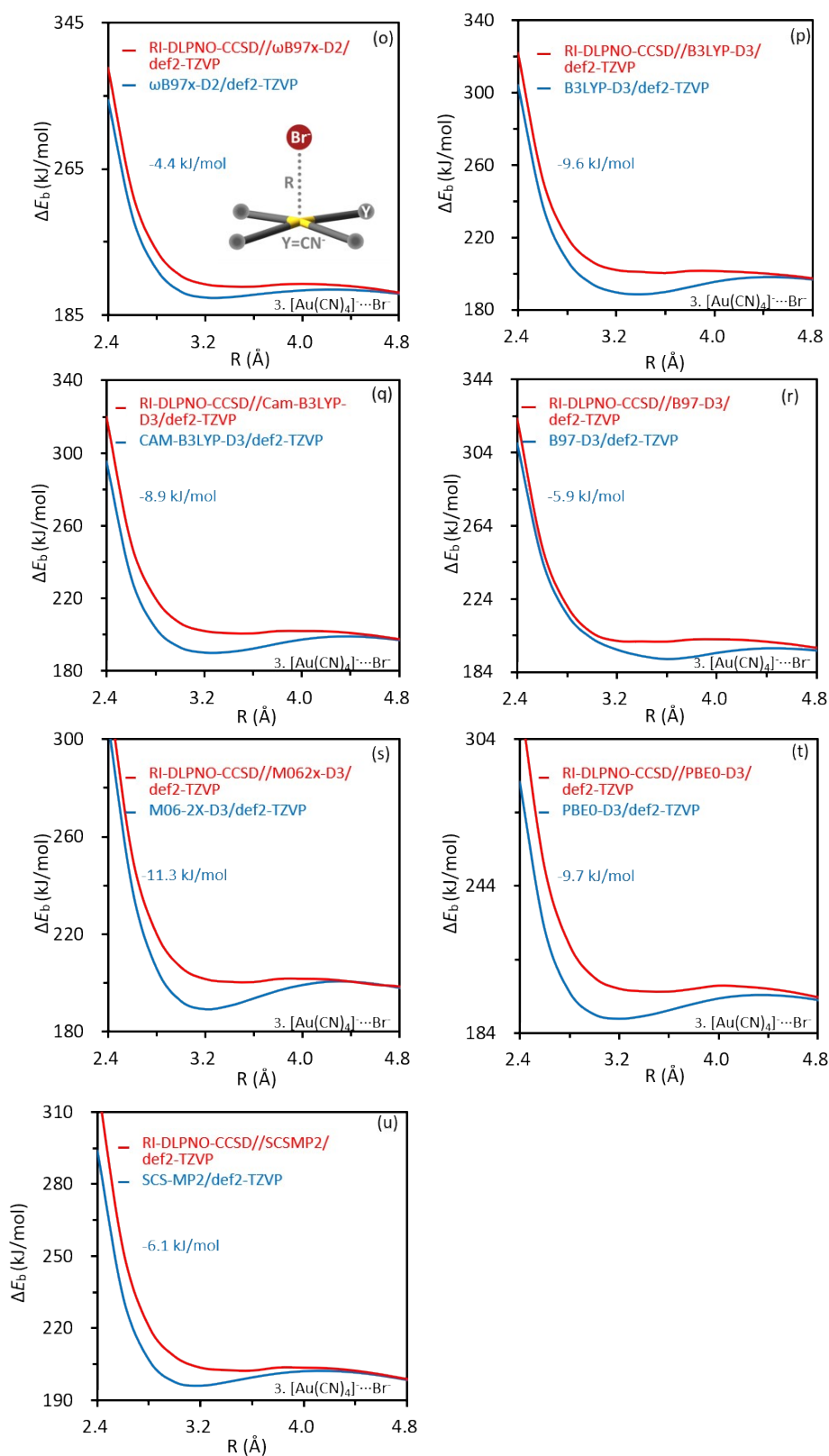
* snnu.changweiwang@snnu.edu.cn; y_mo3@uncg.edu.

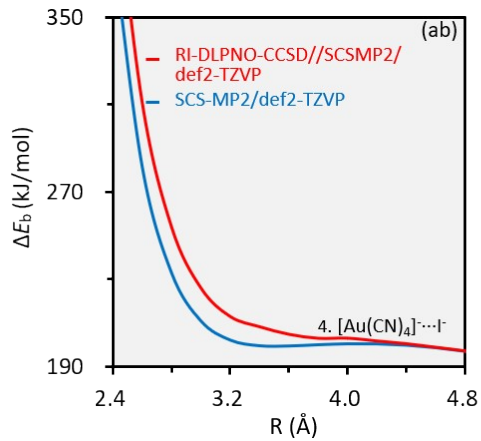
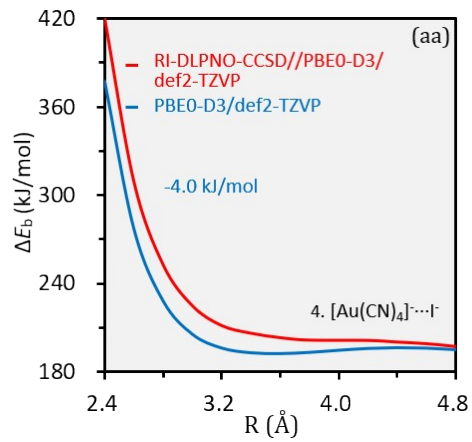
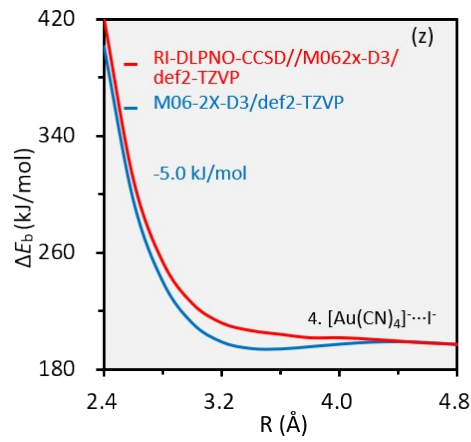
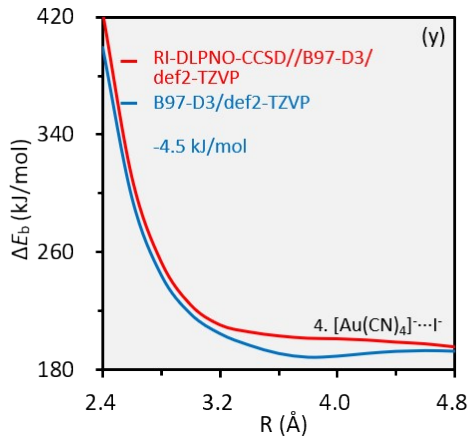
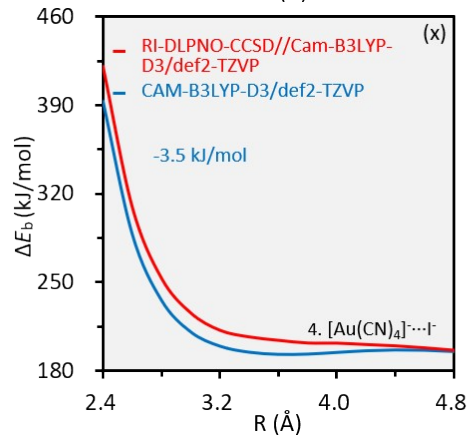
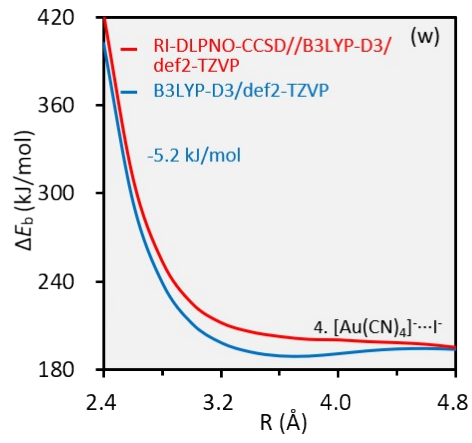
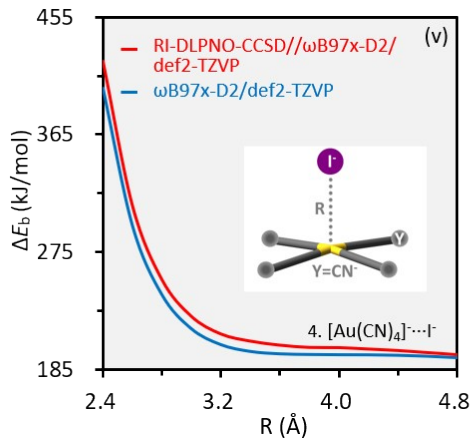
Fig. S1. Profiles of binding energy along the inter-anion distance for complexes 1-6 calculated at a series of theoretical levels.	6
Fig. S2. Profiles of binding energy along with the variation in inter-anion distance calculated at RI-DLPNO-CCSD// ω B97x-D2/def2-TZVP theoretical level. RI-DLPNO-CCSD//def2-QZVPP//SCS-MP2/def2-QZVP theoretical level (s) were also employed for complex $[\text{AuCl}_4]^- \cdots [\text{AuCl}_4]^-$ in order to confirm the absence of metastability.	12
Fig. S3. Evolutions of the inter-anion distance over time (after the 1500st fs) in the AIMD simulation, with the averaged value (R), and the corresponding maximal and minimum deviations denoted.	13
Fig. S4. The electrostatic interaction along the inter-anion distance calculated using the BLW-ED method (in blue) and AMOEBA polarizable force field (in grey).	14
Table S1. Polarizabilities (along the direction of CiBs) of optimized and deformed monomers (α , in a.u.) at ω B97x-D2/def2-TZVP(-PP) theoretical level.	14
Table S2. Amount of charge (ΔQ) transferred from the Lewis base to the acid, calculated using the NPA.	14
Table S3. The distances (\AA) of CiBs in the local minimum (R_{LM}) and transition structure (R_{TS}), and well-depthes (in kJ/mol) derived from the binding energy profiles calculated at RI-DLPNO-CCSD// ω B97x-D2/def2-TZVPD theoretical level.	15
The xyz coordinates (in \AA) of inter-anion CiBs optimized at ω B97x-D2/def2-TZVP level of theory.	15

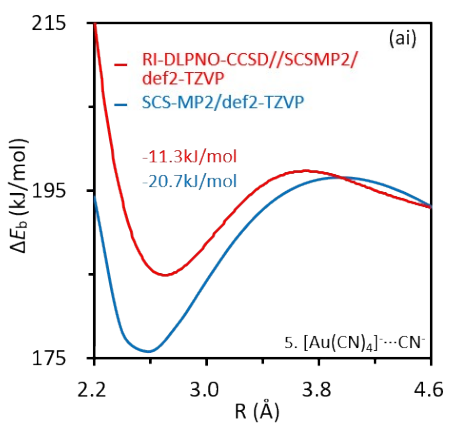
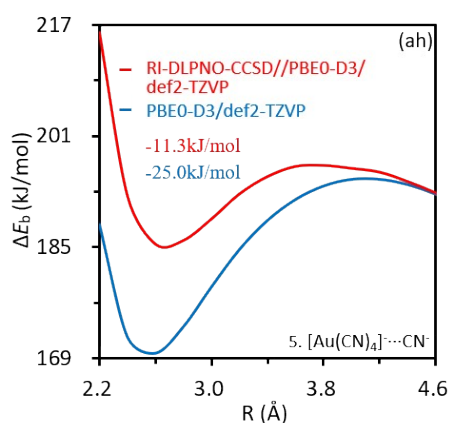
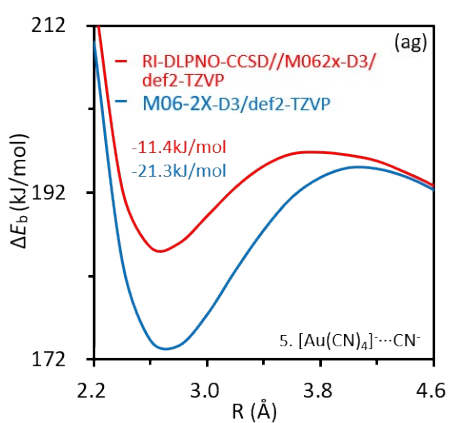
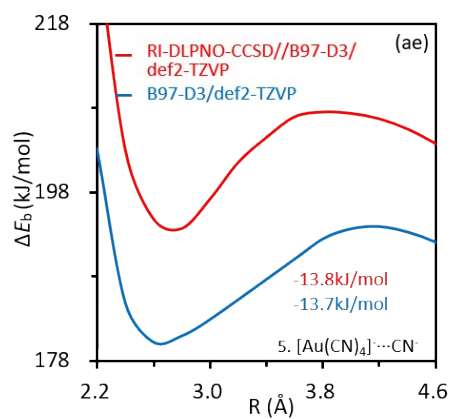
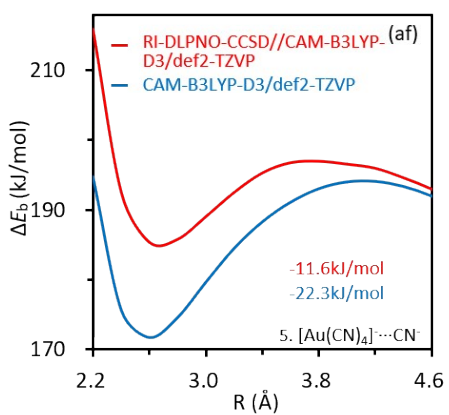
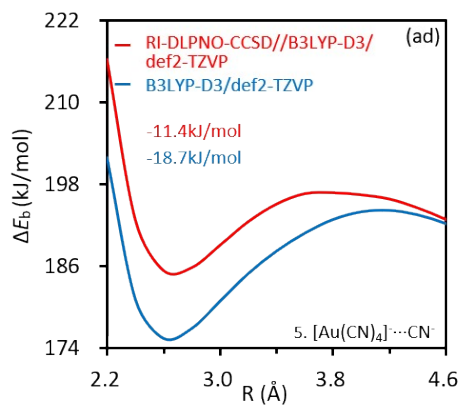
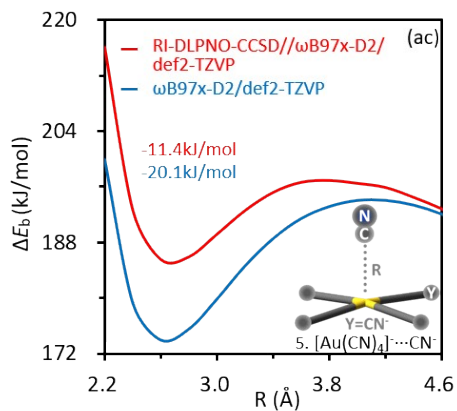
Additional Figures











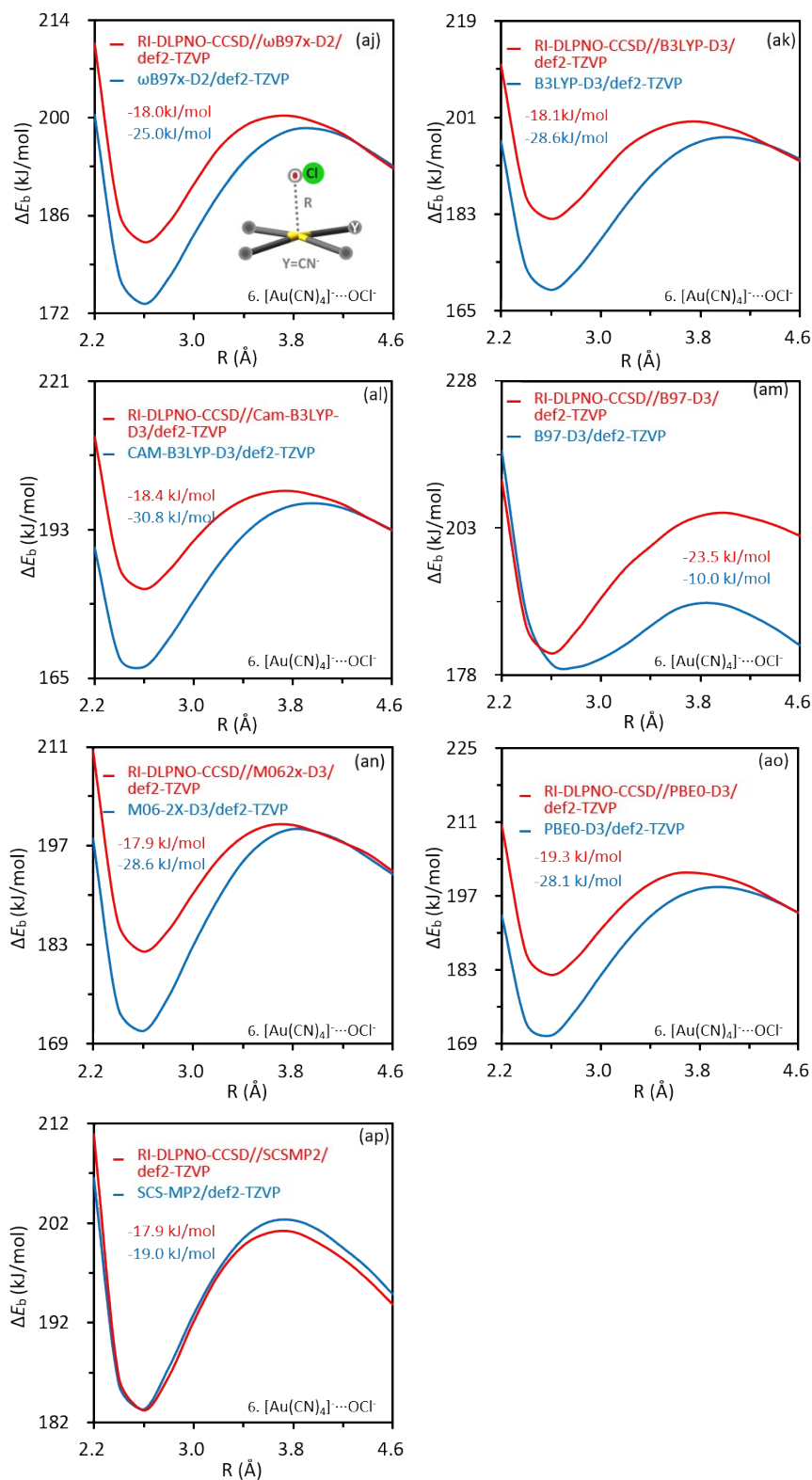
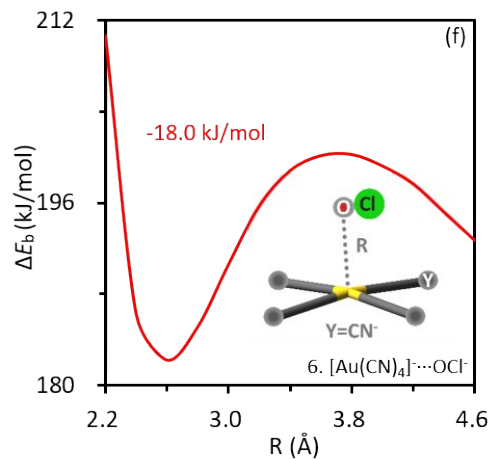
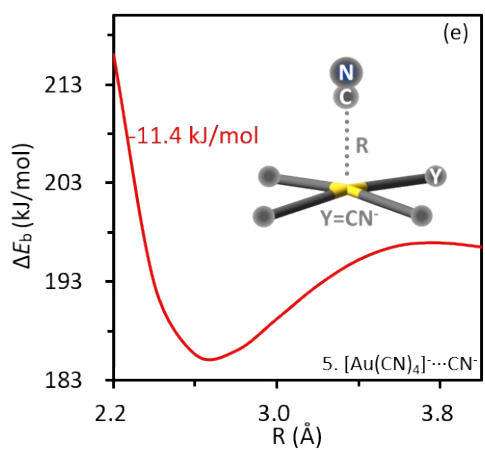
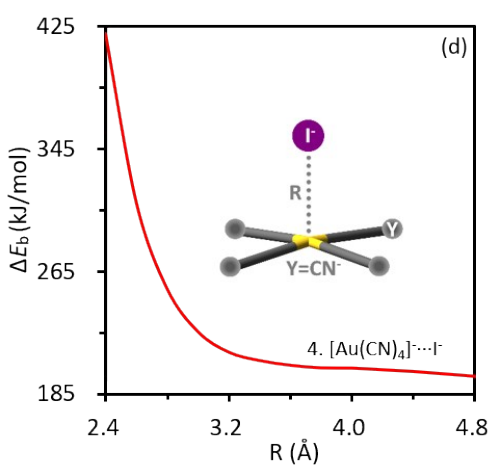
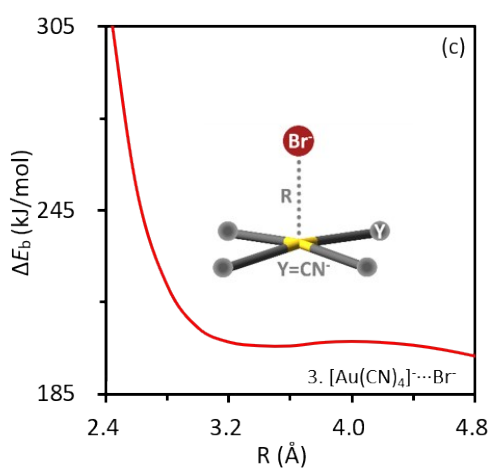
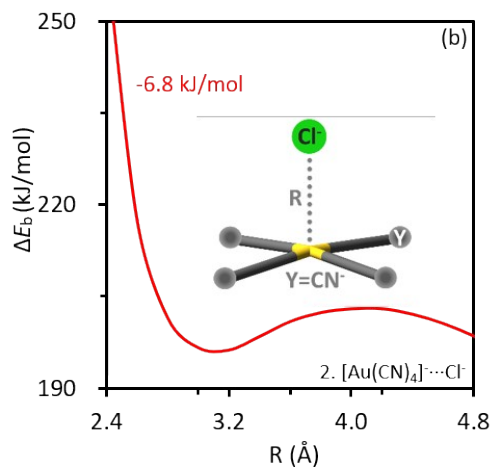
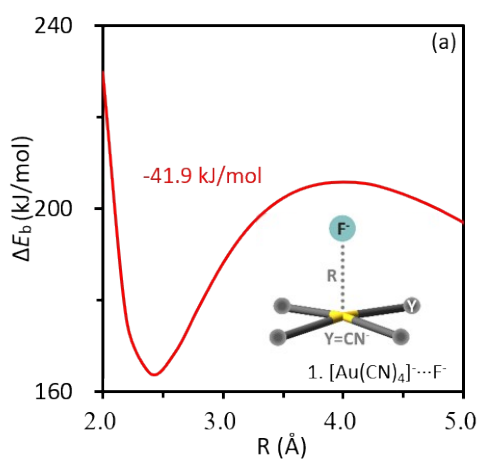
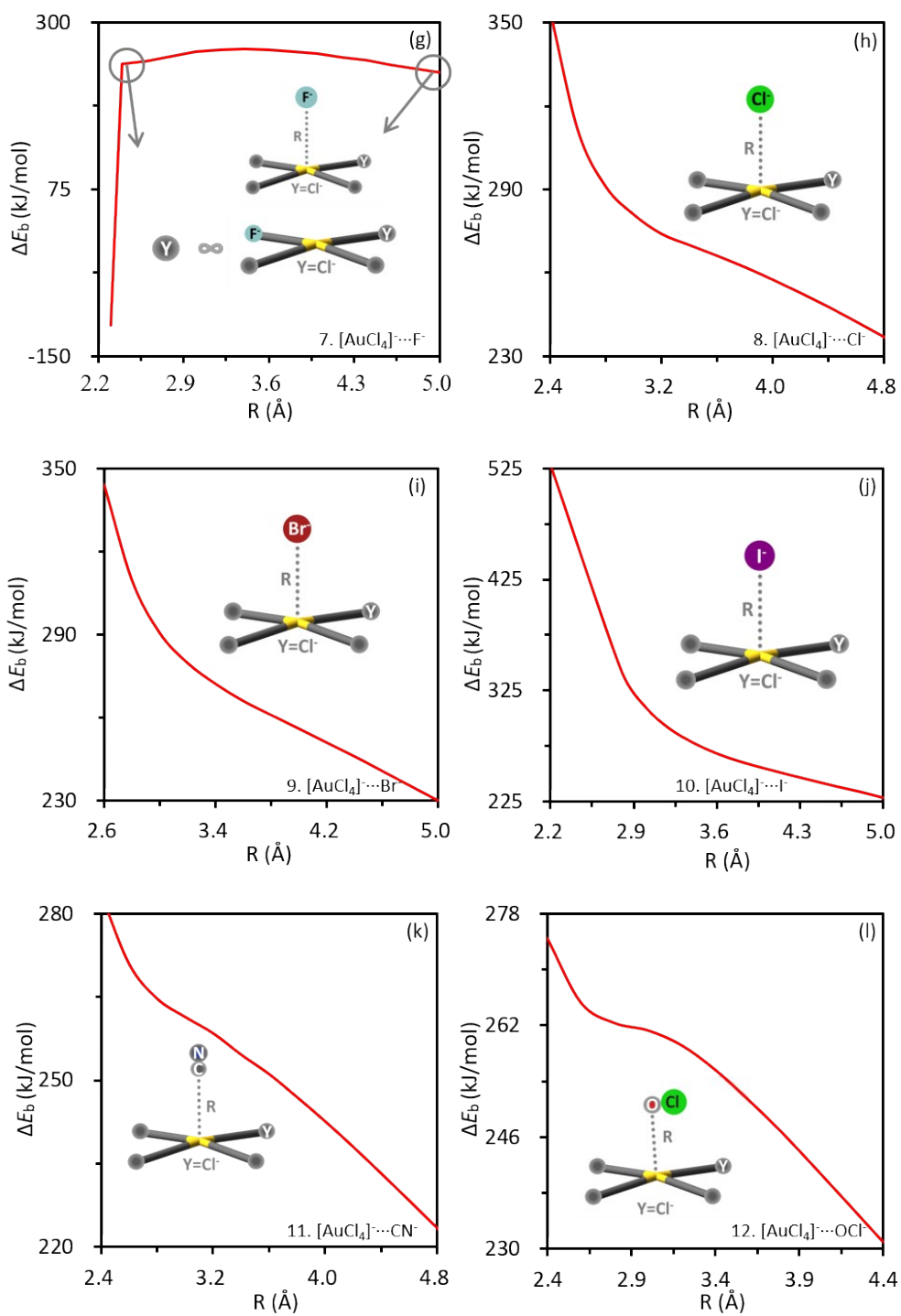
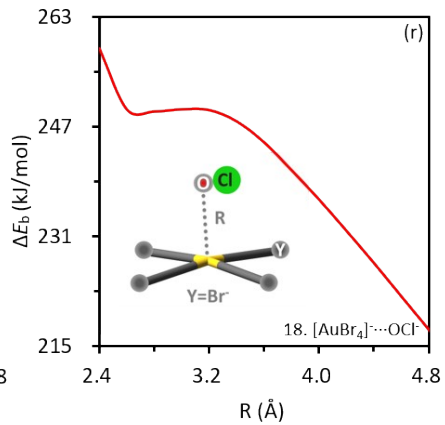
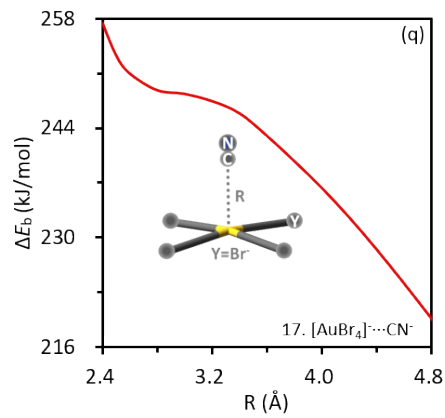
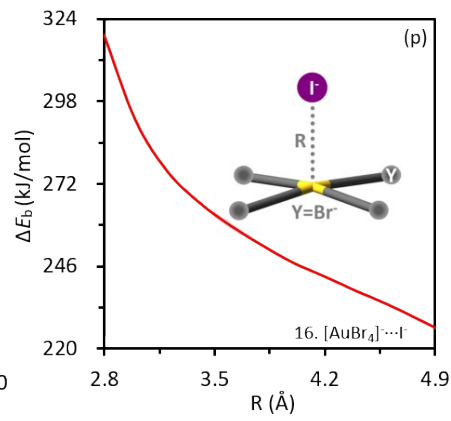
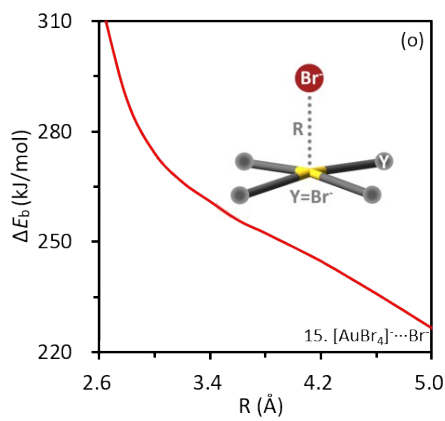
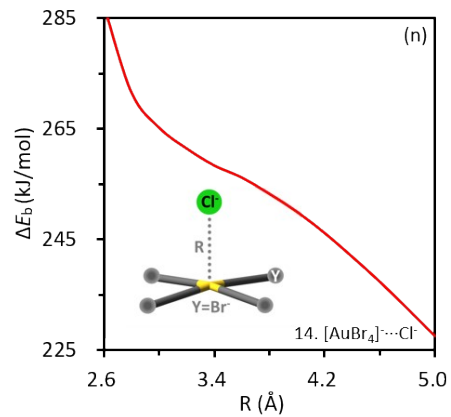
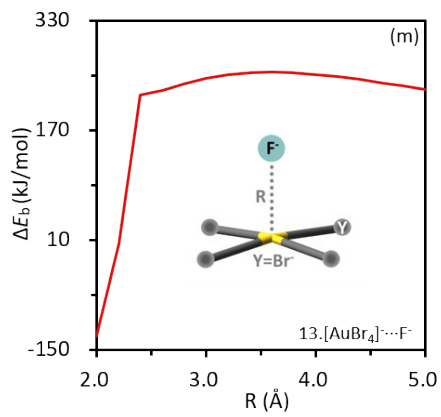
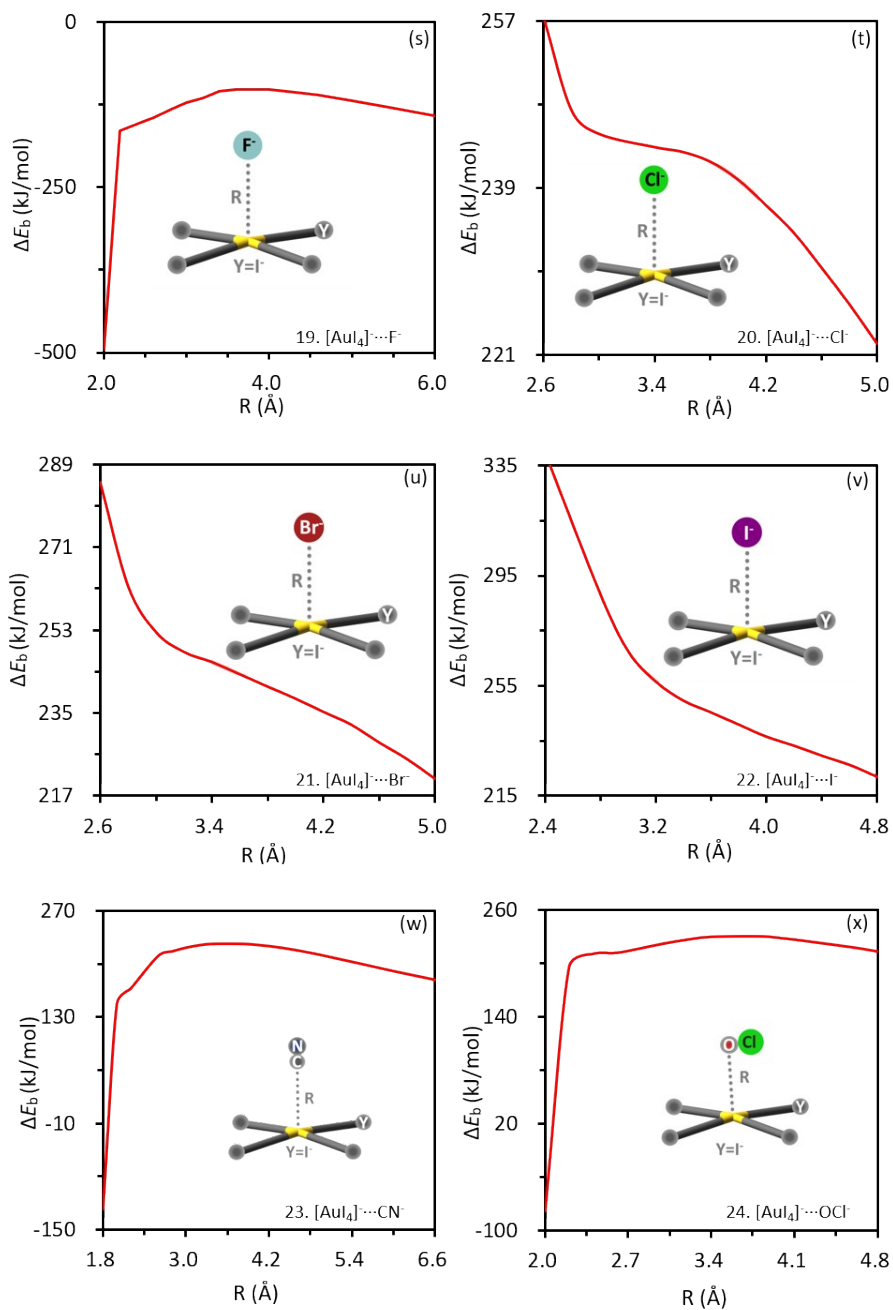


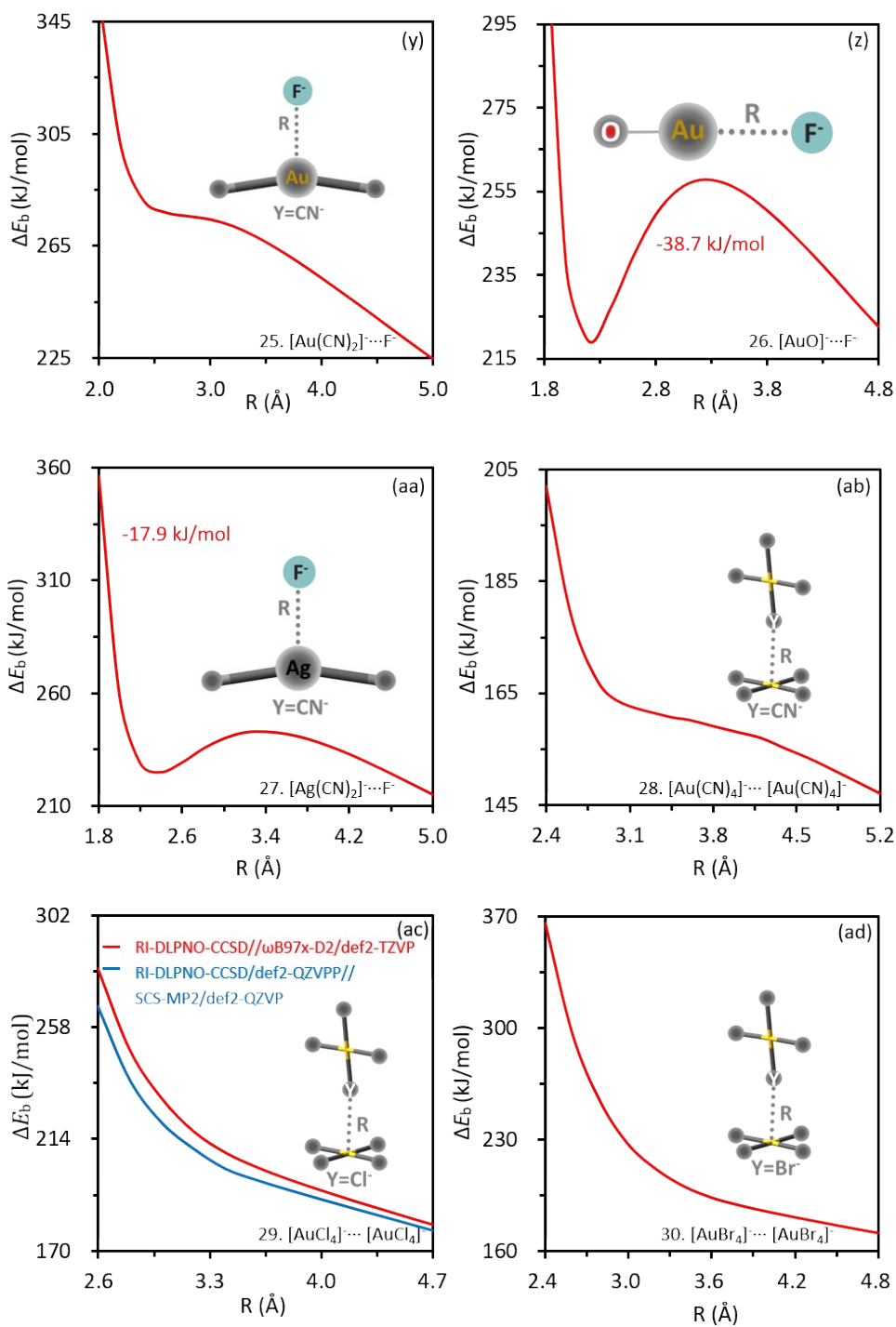
Fig. S1. Profiles of binding energy along the inter-anion distance for complexes 1-6 calculated at a series of theoretical levels.











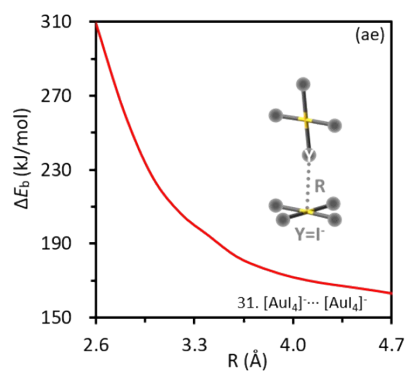


Fig. S2. Profiles of binding energy along with the variation in inter-anion distance calculated at RI-DLPNO-CCSD// ω B97x-D2/def2-TZVP theoretical level. RI-DLPNO-CCSD//def2-QZVPP//SCS-MP2/def2-QZVP theoretical level (s) were also employed for complex $[\text{AuCl}_4]^- \cdots [\text{AuCl}_4]^-$ in order to confirm the absence of metastability.

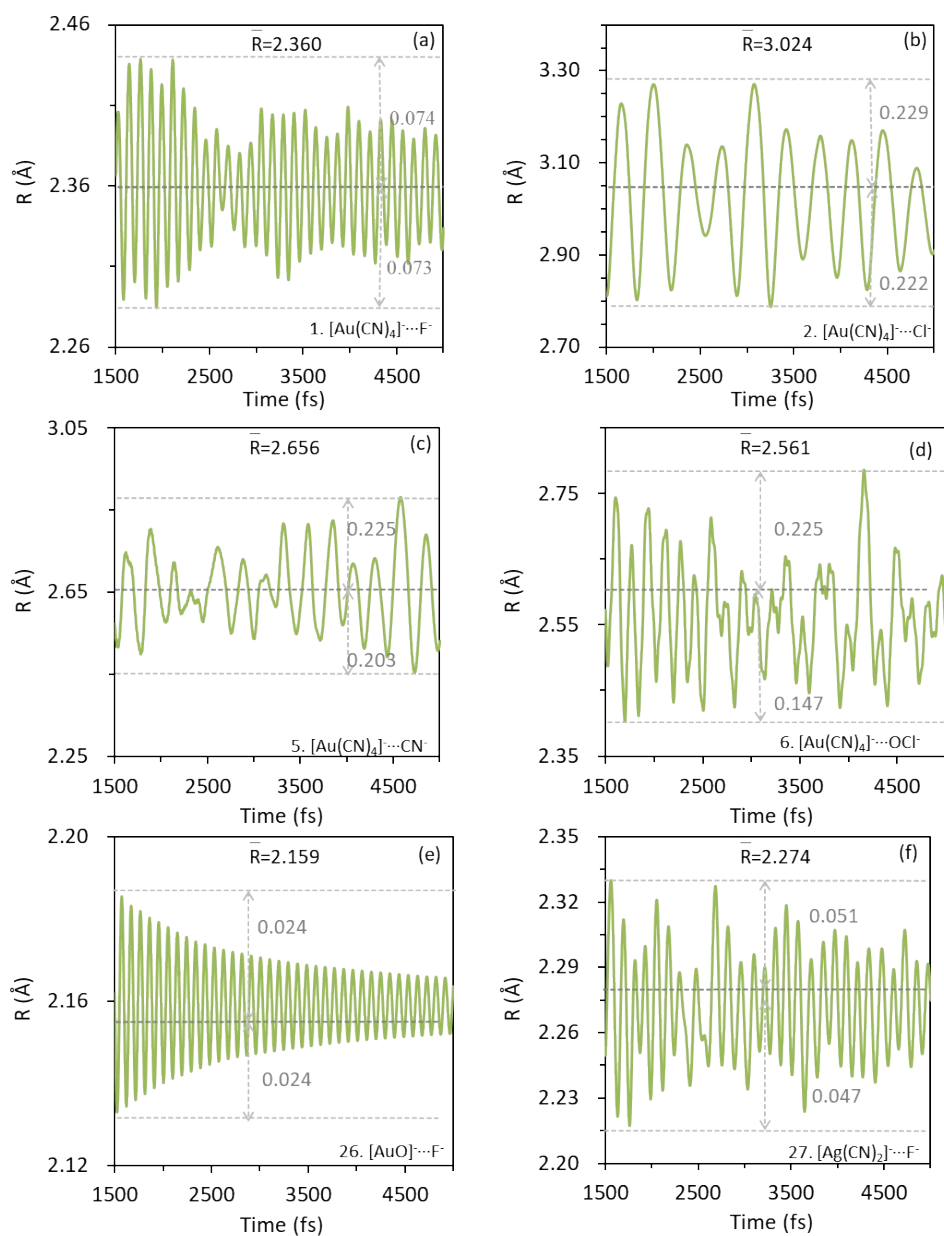


Fig. S3. Evolutions of the inter-anion distance over time (after the 1500st fs) in the AIMD simulation, with the averaged value (\bar{R}), and the corresponding maximal and minimum deviations denoted.

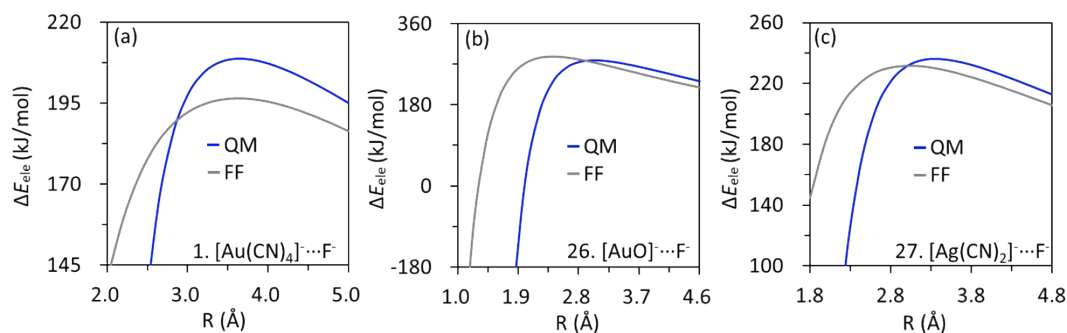


Fig. S4. The electrostatic interaction along the inter-anion distance calculated using the BLW-ED method (in blue) and AMOEBA polarizable force field (in grey).

Additional Tables

Table S1. Polarizabilities (along the direction of CiBs) of optimized and deformed monomers (α , in a.u.) at ω B97x-D2/def2-TZVP(-PP) theoretical level.

No.	Optimized monomer	α	No.	Deformed monomer	α
1	[Au(CN) ₄] ⁻	115.564	1	[Au(CN) ₄] ⁻ ...F ⁻	116.553
2	-	-	2	[Au(CN) ₄] ⁻ ...Cl ⁻	116.070
5	-	-	5	[Au(CN) ₄] ⁻ ...CN ⁻	116.500
6	-	-	6	[Au(CN) ₄] ⁻ ...OCl ⁻	116.238
25	[Au(CN) ₂] ⁻	101.970	25	[Au(CN) ₂] ⁻ ...F ⁻	101.512
26	[AuO] ⁻	71.843	26	[AuO] ⁻ ...F ⁻	73.734
27	[Ag(CN) ₂] ⁻	91.148	27	[Ag(CN) ₂] ⁻ ...F ⁻	85.049

Table S2. Amount of charge (Δ Q) transferred from the Lewis base to the acid, calculated using the NPA.

No.	Complexes	Δ Q	No.	Complexes	Δ Q
1	[Au(CN) ₄] ⁻ ...F ⁻	0.146	6	[Au(CN) ₄] ⁻ ...OCl ⁻	0.122
2	[Au(CN) ₄] ⁻ ...Cl ⁻	0.143	26	[AuO] ⁻ ...F ⁻	0.176
5	[Au(CN) ₄] ⁻ ...CN ⁻	0.258	27	[Ag(CN) ₂] ⁻ ...F ⁻	0.138

Table S3. The distances (\AA) of CiBs in the local minimum (R_{LM}) and transition structure (R_{TS}), and well-depthes (in kJ/mol) derived from the binding energy profiles calculated at RI-DLPNO-CCSD// ω B97x-D2/def2-TZVPD theoretical level.

No.	Complexes	R_{LM}	R_{TS}	$\Delta\Delta E_b$
1	$[\text{Au}(\text{CN})_4]^- \cdots \text{F}^-$	2.400	4.000	-41.3
2	$[\text{Au}(\text{CN})_4]^- \cdots \text{Cl}^-$	3.000	4.200	-8.2
5	$[\text{Au}(\text{CN})_4]^- \cdots \text{CN}^-$	2.800	4.000	-15.5
6	$[\text{Au}(\text{CN})_4]^- \cdots \text{OCl}^-$	2.600	3.800	-18.5
26	$[\text{AuO}]^- \cdots \text{F}^-$	2.200	3.200	-42.2
27	$[\text{Ag}(\text{CN})_2]^- \cdots \text{F}^-$	2.400	3.400	-13.7

The xyz coordinates (in \AA) of inter-anion CiBs optimized at ω B97x-D2/def2-TZVP level of theory.

1. $[\text{Au}(\text{CN})_4]^- \cdots \text{F}^-$

Au	79.0	-0.000461	0.000518	0.206966
C	6.0	0.000034	2.014214	0.047677
C	6.0	2.013240	-0.000035	0.048304
C	6.0	0.000031	-2.013183	0.048338
C	6.0	-2.014157	-0.000038	0.047716
N	7.0	0.000909	3.158170	-0.099547
N	7.0	-3.158109	-0.001022	-0.099543
N	7.0	0.000900	-3.157063	-0.099557
N	7.0	3.157125	-0.001013	-0.099552
F	9.0	-0.007496	0.008431	2.566647

2. $[\text{Au}(\text{CN})_4]^- \cdots \text{Cl}^-$

Au	79.0	-0.001224	0.000091	0.179272
C	6.0	-0.001554	-2.011554	0.030113
C	6.0	2.010583	0.000116	0.032782
C	6.0	-0.001554	2.011710	0.029687
C	6.0	-2.012679	0.000116	0.027058
N	7.0	-0.002046	-3.151602	-0.139194
N	7.0	-3.152482	0.000152	-0.144088
N	7.0	-0.002046	3.151724	-0.139878

N	7.0	3.150845	0.000153	-0.134902
Cl	17.0	-0.000222	0.000016	3.159124

5. $[\text{Au}(\text{CN})_4]^- \cdots \text{CN}^-$

Au	79.0	-0.004488	0.003146	0.191600
C	6.0	-0.003407	2.015299	-0.001183
C	6.0	2.009075	0.002465	0.012521
C	6.0	-0.003501	-2.010101	0.009480
C	6.0	-2.016301	0.002412	-0.004134
N	7.0	-0.002518	3.155430	-0.171118
N	7.0	-3.156148	0.001845	-0.175868
N	7.0	-0.002689	-3.151148	-0.154288
N	7.0	3.150382	0.001950	-0.149264
N	7.0	-0.020218	0.005275	3.975149
C	6.0	-0.015112	0.009541	2.812064

6. $[\text{Au}(\text{CN})_4]^- \cdots \text{OCl}^-$

Au	79.0	0.000867	-0.032056	0.222258
C	6.0	-0.010526	1.982920	0.121511
C	6.0	2.011658	-0.018133	0.054943
C	6.0	0.012383	-2.041277	0.039276
C	6.0	-2.013093	-0.036587	0.102172
N	7.0	-0.014785	3.128968	-0.002469
N	7.0	-3.156243	-0.031735	-0.044925
N	7.0	0.023911	-3.179679	-0.141189
N	7.0	3.152810	-0.005628	-0.107394
O	8.0	0.157767	0.039570	2.751409
Cl	17.0	-0.821687	-0.938053	3.683199

26. $[\text{AuO}]^- \cdots \text{F}^-$

O	8.0	-6.588535	0.261088	0.375474
Au	79.0	-4.691261	0.366706	0.322788
F	9.0	-2.537374	0.472342	0.281211

27. $[\text{Ag}(\text{CN})_2]^- \cdots \text{F}^-$

Ag	47.0	0.015377	0.713246	0.003829
C	6.0	0.001692	-0.074299	2.027078
N	7.0	-0.012517	-0.539432	3.093811
C	6.0	0.002080	-0.064250	-2.021569
N	7.0	-0.012545	-0.529284	-3.088288
F	9.0	0.041293	2.996897	0.017302